České vysoké učení technické v Praze
Fakulta jaderná a fyzikálně inženýrská
Katedra fyziky

Particle confinement of pellet fuelled plasmas in tokamaks

Výzkumný úkol

Autor práce: **Bc. Pavel Háček**
Vedoucí úkolu: **Ing. Martin Valovič, PhD.**
Akademický rok: **2007/2008**

Název práce:
Napouštění paliva do tokamaku vstřelováním pelet a udržení částic v plazmatu

Autor: Pavel Háček

Obor: Fyzikální inženýrství

Druh práce: Výzkumný úkol

Vedoucí práce: Ing. Martin Valovič, Ph.D., EURATOM/ UKAEA Fusion, Abingdon U.K.

Konzultant: Ing. Ivan Ďuran, PhD

Abstrakt: Tokamaky jsou nejpokročilejším zařízením ve výzkumu řízené jaderné fúze. V roce 2007 začala výstavba obřího tokamaku ITER, který má za úkol prokázat technologickou proveditelnost fúze s magnetickým udržením. Jedním z klíčových témat výzkumu je doplňování paliva do tokamaků. Pro velká zařízení jako ITER je nezbytná technologie vstřelování pelet. Pelety ovšem velmi narušují prostředí okraje plazmatu a jsou zdrojem zvýšené aktivity tzv. ELMů a zvýšeného transportu částic a energie. Tento transport se nazývá anomální, neboť neodpovídá teoretickým předpovědím pro difúzi a nabývá mnohem větších hodnot. Část této práce se zabývá teoretickým základem anomální difúze. V druhé části je z experimentálních dat z tokamaku JET kvantifikován transport částic po vstřelení pelet výpočtem difuzního koeficientu a doby udržení peletu.

*Klíčová slova: T*okamak, vstřelování pelet, anomální difúze, difuzní koeficient, doba udržení peletu

Title:
Particle confinement of pellet fuelled plasmas in tokamaks

Author: Pavel Háček

Abstract: Tokamaks are the most advanced devices in the research of controlled nuclear fusion. In the year 2007 construction of giant tokamak ITER has begun. ITER's goal is to demonstrate the technological feasibility of magnetic confinement fusion. One of the crucial parts of the research is the tokamak plasma refuelling. For big devices like ITER, technology of pellet injection is necessary. Pellets, however, disturb the edge plasma and cause enhanced ELM activity along with increased particle and energy transport. This transport is called anomalous, as it does not correspond to theoretical predictions of diffusion and it reaches far higher values. Part of this work is aimed at explaining the theoretical basis of the anomalous diffusion. In the second part, with use of experimental data from the JET tokamak, a post pellet particle transport is quantified by diffusion coefficient and pellet retention time calculation.

Key words: Tokamak, pellet injection, anomalous diffusion, diffusion coefficient, pellet retention time

Contents

1 Introduction

Ongoing research of possible energetic exploitation of a nuclear fusion reactions of light nuclei is now before an important milestone. The most advanced experimental fusion devices are tokamaks, toroidally shaped vacuum vessels where plasma is confined by a strong toroidal magnetic field and weaker poloidal magnetic field. The poloidal magnetic field in tokamaks is produced by an induced plasma current. After succesful demonstration of physical feasibility of fusion by large tokamaks like JET, the need of a larger device capable of demonstrating the technological feasibility of fusion and provide the necessary data to design and operate the first electricity-producing fusion power plant has arisen. In the year 2007, the construction of ITER (international thermonuclear experimental reactor) tokamak has begun. ITER is an international project of seven participants: The European Union (represented by EURATOM), Japan, The People's Republic of China, India, the Republic of Korea, the Russian Federation and the USA. The construction costs of ITER are estimated at five billion Euro and another five billion Euros are estimated for its 20-year long operation, thus making it one of the most expensive research projects of our time. Its objectives are to achieve a steady-state burn of deuterium-tritium plasma producing 500MW of fusion power, achieve the power amplification factor Q = 10 and testing of the inner components facing high-heat and neutron fluxes. It should start its operation by the end of the year 2016. [1]

Plasma refuelling is one of the most important and fundamental parts of the tokamak research. It is desirable to deliver the fuel particles to the core plasma and confine them for as long as possible. With the necessity of increasing the tokamak dimensions and plasma temperature it is more difficult to deliver the fuel particles deep into the plasma column. Simple gas puff used for the smaller tokamaks becomes incapable of that task and is therefore inefficient. The most important technology of tokamak plasma fuelling for future devices like ITER would be *pellet injection*. Small (1-6mm diameter) solid fuel pellets are injected at high speeds of hundreds of meters per second into the plasma. It penetrates deeper into the plasma and is therefore generally more efficient than gas puffing. The fuel particle confinement improves, because it takes a longer time for a deeper delivered particles to escape from the magnetic trap diffusively. In experiments, energy and particle confinement has been observed to improve along with enhancement of thermonuclear reactivity. The pellet injection also allows us to operate at higher densities and to better control the shape of the plasma density profile. [2]

The question of refuelling is also closely connected with the energy and particle confinement and transport in plasma. Magnetic confinement of the hot plasma particles in tokamaks is not perfect. The confinement of the toroidally symmetric tokamak plasma has been calculated for particle Coulomb collisions. This so called *neoclassical transport* does not, however, agree with the experiments. In particular the thermal transport by electrons can be up to two orders of magnitude grater than predicted by neoclassical theory. It is believed that this observed *anomalous transport* occurs because of plasma instabilities. To explain and understand the theory of anomalous transport is one of the major challenges for present tokamak physics. [3]

This work is based upon previous bachelor thesis [2]. In [2] a post pellet particle diffusion coefficient is calculated and basics of tokamak transport physics is given. This work's goal was to

attempt to improve the calculation of the post pellet diffusion coefficient, translate the result to a pellet particle confinement time and provide the basics of anomalous particle and heat transport in tokamaks and relate to situation of pellet fuelling. In this work, a data from JET tokamak shot 53212 are used.

2 Transport in tokamaks

2.1 Introduction

To achieve thermonuclear conditions in tokamaks, it is necessary to contain it for a sufficiently long time. An important parameter describing the confinement is the global energy confinement time, defined as:

$$\tau_E = \frac{1}{P}\int \frac{3}{2} k\left(T_i + T_e\right) d^3x \ , \qquad (2.1)$$

where n is plasma density, T_i and T_e ion and electron temperature, k the Boltzmann constant and P is total power input. The integral is taken across the plasma volume. The plasma confinement is limited by outward heat and particle transport and radiation.

If we assume cylindrical geometry of the plasma and consider Coulomb collisions only, we get so called *classical transport*. This approach is not accurate, as we do not consider important toroidal effects. Calculation of the transport in toroidal geometry, including particle trapping and various drifts is a *neoclassical approach*. Unfortunately, the transport which occurs in tokamaks usually does not agree with the calculated neoclassical values. It reaches far greater values, especially the electron heat transport, which can be up to two orders of magnitude higher. It is believed that this amplified transport is driven by turbulence caused mainly by plasma micro-instabilities, which allow the particles to escape at a higher rate. These turbulence processes are hihly non-linear, there are multiple turbulence drives and supression mechanisms, which occur on multiple scales. The complexity of this problem has made the understanding of tokamak transport a very difficult task. Understanding the anomalous transport is one of the most important issues of present and future fusion reactors. [3],[5]

2.2 Transport equations and transport coefficients

Transport phenomena (transport of particles, momentum, energy...) are caused by the collision processes in plasma. If the system is deviated from the thermodynamical equilibrium, macroscopic fluxes appear, which tend to recover the equilibrium. These fluxes are driven by gradients of thermodynamic quantities (these gradients are called thermodynamic forces) and generally, one thermodynamic force may cause more types of macroscopical fluxes. In our case, the particle and heat flux is considered: We define the particle flux Γ as the number of particles passing through a magnetic surface per unit of area per unit of time and the heat flux q as the flow of energy per unit of area per unit of time. A simplified equations for these fluxes in tokamaks are often used:

$$\Gamma_j = -\alpha_{11}\nabla n_j - \alpha_{12}\nabla T_j, \quad (2.2)$$

$$q_j = -\alpha_{21}\nabla n_j - \alpha_{22}\nabla T_j, \quad (2.3)$$

where T_j is the temperature of the species j and n_j is the density of the species j. In (2.2), (2.3) it is assumed that a flux for a specific species depends on temperature and density gradients of that species only and another gradients (like electric potential gradient etc.) are not considered. The relation of the fluxes on the gradients is then described by a matrix of coefficients (α_{ij}). The diagonal elements of the matrix are the usual D_j and $n\chi_j$, where D_j is the diffusion coefficient and χ_j is the thermal diffusion coefficient (thermal conductivity). Note that in anisotropic magnetized tokamak plasma these diffusion coefficients are tensors themselves. Sometimes the particle flux Γ is expressed in alternative simplified forms:

$$\Gamma_j = -D\nabla n_j - vn_j \text{ or } \Gamma_j = -D_{eff}\nabla n_j \quad (2.4), (2.5)$$

which says that it has a diffusive part driven by a density gradient and characterized by the diffusion coefficient D and a convective part with a velocity v. The convective part then represents the contribution of the off-diagonal terms of the matrix in (2.2), (2.3). If the velocity v is positive, then this term describes an inward pinch. In (2.5) both diffusion and convection process are described by an effective diffusion coefficient, as it is usually difficult to distinguish them.

With use of the equation (2.4), the equation of continuity and the Gauss law it is possible to derive the diffusion equation [2]:

$$\frac{\partial n}{\partial t} = \nabla \cdot (D\nabla n) + \nabla(nv) + S, \quad (2.6)$$

where S is a source term describing the change of plasma density due to ionisation or recombination S. [2],[3],[6],[7]

The typical diffusivities measured on tokamaks are:

- $\chi_i, \chi_e \sim 1\ m^2s^{-1}$
- $D \sim ¼\ \chi_e$

where D is a diffusion coefficient (same for both species as the diffusion is ambipolar). The typical neoclassical values for diffusivities are generally much lower:

- $\chi_{i,neo} \sim 0.3\ m^2s^{-1}$
- $\chi_{e,neo} \sim D_{neo} \sim (m_e/m_i)^{1/2}\chi_{i,neo}$

Therefore generally

- $\chi_i \sim 1\text{-}10\ \chi_{i,neo}$

- $\chi_e \sim 10^2 \chi_{e,neo}$
- $D \sim 10\text{-}10^2 D_{neo}$

In experiments, the values of D, χ_i can approach the neoclassical values in the plasma core region or during a high confinement operation (H-mode, internal transport barrier...), but χ_e is almost always anomalous.[3]

2.3 Anomalous transport

The turbulence-driven anomalous transport is caused by fluctuations in the plasma. These fluctuations may be electrostatic or electromagnetic and are supposed to be an effect of one or more microinstabilities of the tokamak plasma. Macroscopic MHD instabilities like sawteeth, magnetic islands or ELMs are also an important source of the anomalous transport.

For a fluctuating quantity f we may write:

$$f = \langle f \rangle + \delta f, \tag{2.7}$$

where < > means averaging over a flux surface. The turbulent fluctuations result in *ExB drift* velocity δv_{perp} perpendicular to the flux surface:

$$\delta v_{perp} = \delta E_{perp} / B_T, \tag{2.8}$$

where δE_{perp} is electric field fluctuation perpendicular to the flux surface and B_T is toroidal magnetic field. This velocity along with density fluctuations δn combine to produce a convective particle flux Γ:

$$\Gamma = \langle \delta v_{perp} \, \delta n \rangle, \tag{2.9}$$

where < > means again averaging over a flux surface. The particle flux (2.9) must be then averaged also in time as the fluctuations are also time-dependant. The time average must be done over a time interval higher than all characteristic times in the plasma (electron and ion plasma frequency, electron and ion cyclotron frequency...). Therefore the time and space correlation between fluctuations plays an important role. This equation (2.9) will be nonzero except a situation of δv_{perp}, δn being exactly out of phase. For a turbulent heat flux the temperature fluctuations δT_j play a role:

$$q_j = 3/2 \, n_j \langle \delta v_{perp} \, \delta T_j \rangle, \tag{2.10}$$

where n_j is an equilibrium density and index j denote the species. In case of magnetic fluctuations δB associated with a change in magnetic topology, the perturbed velocity δ_{pae} parallel to the magnetic field along with a perturbed radial magnetic field δB_r give rise to a flux:

$$\Gamma_j = (n_j / B_T) \langle \delta v_{par,j} \, \delta B_r \rangle. \tag{2.11}$$

The fluctuations in δn, δT_e and the electric potential $\delta\phi$ at the edge plasma can be measured by Langmuir probes and the magnetic fluctuation δB can be measured by Mirnov coils. It is observed, that $\delta n/n$, $\delta T_e/T_e$ and $e\delta\phi/kT_e$ rise quickly towards the plasma edge, where they can reach values ~50%. On the other hand the edge plasma value of $\delta B/B$ is usually small, typically ~10^{-4}. The internal density fluctuations can be much lower falling to ~1%. The plasma potential fluctuations in the core follow approximately a relation $e\delta\phi/kT_e \sim \delta n/n$.

It is usual to perform a spatial fourier transform of the fluctuations and observe the wavenumbers k_{perp} and k_{par} perpendicular and parallel to the magnetic field. The spectrum $S(k_{perp})$ is dominated by wavelengths (wavelength $\lambda=2\pi/k$) greater than the ion Larmor radius $r_{L,i}$. In radial direction the spectrum is peaked at the longest wavelength measurable. In the azimuthal (poloidal) direction, the spectrum is peaked in the region $k_{perp}\cdot\rho_s \leq 0.3$, where ρ_s is the ion Larmor radius at the electron temperature. For spectrum $S(k_{par})$ of wavenumbers parallel to the magnetic field, the typical values are $k_{par}\cdot L \sim 1$, where L is connection length around the torus ($L=qR$, where q is the safety factor and R major radius). The characteristic frequencies of the fluctuations are ~ *100kHz*. [3]

Electrostatic fluctuations

As was mentioned in the previous paragraph, it is usual to perform a Fourier transform of the fluctuations $\delta f(t,\vec{x}) \leftrightarrow \delta f_k(\omega,\vec{k})$:

$$\delta f(t,\vec{x}) = \sum_k \delta f_k e^{i\left(\vec{k}\vec{x}-\omega_k t\right)}, \tag{2.12}$$

where $\boldsymbol{k}$ is the wavenumber (wave vector) and ω_k is the angular frequency. If the electrostatic potential fluctuation $\delta\phi$ is present, it causes ExB drift velocity $\delta\boldsymbol{v}$. For particular component $\delta\phi_k$ this velocity may be written as:

$$\delta\vec{v}_k = -i\frac{\delta\phi_k}{B}\vec{k}. \tag{2.13}$$

and its component perpendicular to the magnetic field **B** as:

$$\delta\vec{v}_{k,perp} = -i\frac{\vec{k}\times\vec{B}}{B^2}\delta\phi_k. \tag{2.14}$$

If this particle velocity persists for a so called *correlation time* τ_k, it leads to a radial displacement of a particle $\delta r_k \sim \delta v_{k,perp}\tau_k$. A random walk estimate for the turbulent diffusion driven by electrostatic fluctuations is then given as:

$$D = \sum_k \frac{\left(\delta r_k^2\right)}{\tau_k} = \sum_k \left(\frac{k_{perp}\delta\phi_k}{B}\right)^2 \tau_k. \tag{2.15}$$

The correlation time is determined by the process which most rapidly limits the radial drift velocity $\delta v_{k,perp}$. The main possible processes determining τ_k are:

a) The time variation of the fluctuation determined by ω_k: $\tau_k \sim 1/\omega_k$.
b) The time for a particle to move along a parallel wavelength of the fluctuation: $\tau_k \sim 1/k_{par}v_{par}$.
c) The time for magnetic drifts (drifts of magnetic field lines) to carry the particle along a perpendicular wavelength of the fluctuation: $\tau_k \sim 1/\omega_d$.
d) The time for collisions to change the particle orbit: $\tau_k \sim 1/\nu$, where ν is the collision frequency of particles.
e) The time for a turbulent velocity δv_k to carry the particle along a perpendicular wavelength: $\tau_k \sim 1/\Omega_k$, where $\Omega_k = k_{perp}\delta v_k$.

Therefore for a low level of fluctuations $\Omega_k \ll \omega_{eff,k}$, where $\omega_{eff,k} = max(\omega_k, k_{par}v_{par}, \omega_d, \nu)$, the equation (2.15) can be rewritten as:

$$D = \sum_k \frac{1}{\omega_{eff,k}} \left(\frac{k_{perp}\delta\phi_k}{B} \right)^2 , \tag{2.16}$$

and therefore $D \propto (\delta\phi)^2$. For higher level of fluctuations $\Omega_k \geq \omega_{eff,k}$ the equation (2.15) can be rewritten as:

$$D = \sum_k \frac{\delta\phi_k}{B} \tag{2.17}$$

and so $D \propto \delta\phi$. [3]

Magnetic fluctuations

Magnetic fluctuations $\delta\boldsymbol{B}$ affect the structure of the magnetic surfaces and can produce ergodic magnetic fields. The motion of plasma particles along these magnetic field lines may then lead to their radial transport and losses. A radial magnetic field perturbation δB_r at a rational surface at radius r_{mn}, where the safety factor $q=m/n$ (m,n are identified as poloidal and toroidal mode), leads to a creation of a magnetic island of width:

$$w_{mn} = \sqrt{\frac{L_s r_{mn}}{m} \frac{\delta B_r}{B}} , \tag{2.18}$$

where $L_s = Rq^2 / rq'$ is called the magnetic shear length, R is the major radius and r is the minor radius. With increasing level of the magnetic fluctuations, an increasing part of the regions between resonant surfaces becomes ergodic. This behaviour is quantified by a parameter:

$$\alpha = \frac{\sum_{m,n} w_{m,n}}{\Delta r}, \tag{2.19}$$

where the sum is over all modes *m, n* with rational surfaces in interval of radii Δr. When $\alpha \gg 1$ many islands overlap and the behaviour of the magnetic field lines becomes stochastic. In this case a radial diffusion of the field lines can be described by a magnetic field line diffusion coefficient D_M. If the radial field perturbation remains in the same direction over a so called *correlation length* L_c, then the field line takes a radial step:

$$\delta r \approx \frac{\delta B_r}{B} L_c . \tag{2.20}$$

A random walk estimate for the magnetic field line diffusion coefficient can be made as:

$$D_M = \sum_k \frac{(\delta r_k)^2}{L_{ck}} = \sum_k \left(\frac{\delta B_{rk}}{B} \right)^2 L_{ck} . \tag{2.21}$$

For a weak turbulence the correlation length $L_{ck} \sim 1/k_{par} \sim Rq$ and $D_M \propto (\delta B_r)^2$.

Assuming collisionless plasma, where the mean free path exceeds the correlation length $\lambda > L_c$, a particle can move freely along the radially diffusing magnetic field line with velocity v_{par} for a collision time τ_c. So it makes a radial step $\delta r = \sqrt{D_M \lambda}$. The diffusion coefficient for particles can be then estimated as:

$$D = \frac{(\delta r)^2}{\tau_c} = \frac{D_M \lambda}{\tau_c} = v_{par} D_M . \tag{2.22}$$

For a more collisional plasma, where $\lambda < L_c$ the particle collisionally diffuses along the magnetic field lines with a radial step $\delta r \sim (\delta B_r/B)\lambda$ in a collision time τ_c. The diffusion coefficient for particles can be in this case estimated as:

$$D = \left(\frac{\delta B_r \lambda}{B} \right)^2 \frac{1}{\tau_c} = D_{par} \left(\frac{\delta B_r}{B} \right)^2 , \tag{2.23}$$

where $D_{par} = (\lambda^2/\tau_c)$ is the collisional diffusion coefficient parallel to the magnetic field lines. [3]

3 Experimental results

3.1 Experimental setup

The data evaluated in this work are from the JET shot 53212, which was a part of experiments undertaken at JET aimed to develop optimized pellet refuelling scenarios.

The basic parameters of the JET 53212 pulse are given in the *Tab.1* below:

Plasma current I_p	*2.5 MA*
Toroidal magnetic field B_t	*2.4 T*
Major radius R	*2.96 m*
Minor radius a	*0.92 m*
Elongation κ	*1.7*
Edge safety factor q_{95}	*3.2*
Plasma volume V_p	*80 m^3*
Plasma averaged triangularity $<\delta>$	*0.34*
Additional plasma heating P_i	*17 MW NBI, 1 MW ICRH*

Table1: Summary of the basic parameters for JET pulse number 53212

The basic parameters of the pellets and the pellet injection system:

Pellet size	4 *mm^3*, $3 \cdot 10^{21}$ atoms
Composition	deuterium
Repetition rate	3Hz, 6Hz
Injection speed	160 *$m \cdot s^{-1}$*
Injection path	from HFS along a trajectory tilted by 44° to the horizontal plane.

Table2: Summary of the basic pellet parameters for JET pulse number 53212

More detailed information about the discharge can be found in [2].

3.2 Diffusion coefficient

An important goal of this work was to try to determine the post pellet diffusion of particles more accurately and provide a more profound analysis of the process, than was done in [2]. In [2] in order to quantify the particle diffusivity after the pellet, the diffusion coefficient was estimated. A boxcar method was applied, in order to cope with insufficient time resolution of the density profile measurement of the LIDAR diagnostics on JET. For a numerical calculation of diffusion coefficient from discrete experimental data, the derivatives in the simplified diffusion equation

$$\frac{\partial n}{\partial t} - D\Delta n = 0 \tag{3.1}$$

were approximated by differences and the value of the effective diffusion coefficient (covering both the diffusion and the convection processes) was determined as $D_{eff} = 0.8 \pm 0.4\ m^2 s^{-1}$. (from now on, by the diffusion coefficient we mean its effective value).

In this work, a more accurate analysis was done by fitting the experimental post pellet density evolution data by a function, which is a mathematical correct solution of the diffusion equation. Still, the data preprocessed by the boxcar analysis in [2] were used.

The simplified diffusion equation (3.1) is a parabolic partial differential equation, which is very important in the mathematical physics. Generally an equation of this particular shape is called the heat equation, as the same equation is used to describe a distribution of heat in a given region over time. The general form of the heat equation in n-dimensional Euclidean space E^{n+1} is following:

$$\frac{\partial n}{\partial t} - a\sum_{k=1}^{n}\frac{\partial^2 n}{\partial x_k^2} = f(\vec{x},t), \tag{3.2}$$

where a is a constant, $f(\mathbf{x},t)$ is the source term and $n(\mathbf{x},t)$ is the mass density. This equation (3.2) together with an initial condition:

$$n(\mathbf{x},0) = \alpha(\mathbf{x}) \tag{3.3}$$

is called *the classical Cauchy problem for the heat equation*. It can be generally solved by transforming it to a *generalized Cauchy problem for the heat equation:*

$$\frac{\partial n}{\partial t} - a\sum_{k=1}^{n}\frac{\partial^2 n}{\partial x_k^2} = \theta(t)f(\vec{x},t) + \delta(t)\alpha(\vec{x}), \tag{3.4}$$

where $\Theta(t)$ is Heaviside step function of time and $\delta(t)$ is the Dirac delta function of time. Another step is finding the fundamental solution $\varepsilon(\mathbf{x},t)$ for the heat conduction operator L:

$$L = \frac{\partial}{\partial t} - a\cdot\Delta \tag{3.5}$$

in a space E^{n+1}. The general solution of the classical Cauchy problem for the heat equation is then determined by a convolution of the fundamental solution $\varepsilon(\mathbf{x},t)$ and the right side of the generalized equation (3.4):

$$n(\vec{x},t) = \int_0^t\int_{R^n}\frac{f(\vec{\xi},t)}{\left(2\sqrt{\pi a(t-\tau)}\right)^n}e^{-\frac{\|\vec{x}-\vec{\xi}\|^2}{4a(t-\tau)}}d\vec{\xi}\,d\tau + \int_{R^n}\frac{\alpha(\vec{\xi})}{\left(2\sqrt{\pi at}\right)^n}e^{-\frac{\|\vec{x}-\vec{\xi}\|^2}{4at}}d\vec{\xi}\,. \tag{3.6}$$

This equality (3.6) is sometimes called *the Poisson formula*. [8],[9]

In our particular case, the diffusion (heat) equation is homogenous, without the source term $f(x,t)$ and the constant a is equal to the diffusion coefficient D. The initial condition $n(x,0)=\alpha(x)$ is the density profile just after the pellet injection into the plasma, at the beggining of decay process of pellet induced perturbation. The form of the general solution (3.6) is then reduced to the second term only (the first integral being zero because of the lack of the source term f). This form of the solution of our diffusion equation is however still rather difficult. For the further described analysis, solutions of the simplified form of the heat equation in axial symmetry was used.

According to [10], two ways were used in this work to estimate the post pellet diffusion coefficient.

- Gaussian fit analysis
- Bessel functions analysis.

The data used were three post pellet density profiles in relative times (to the time of pellet injection), which come out from the boxcar analysis in [2]. These profiles along with the pre-pellet density profile, are given on *Fig.3.1* below.

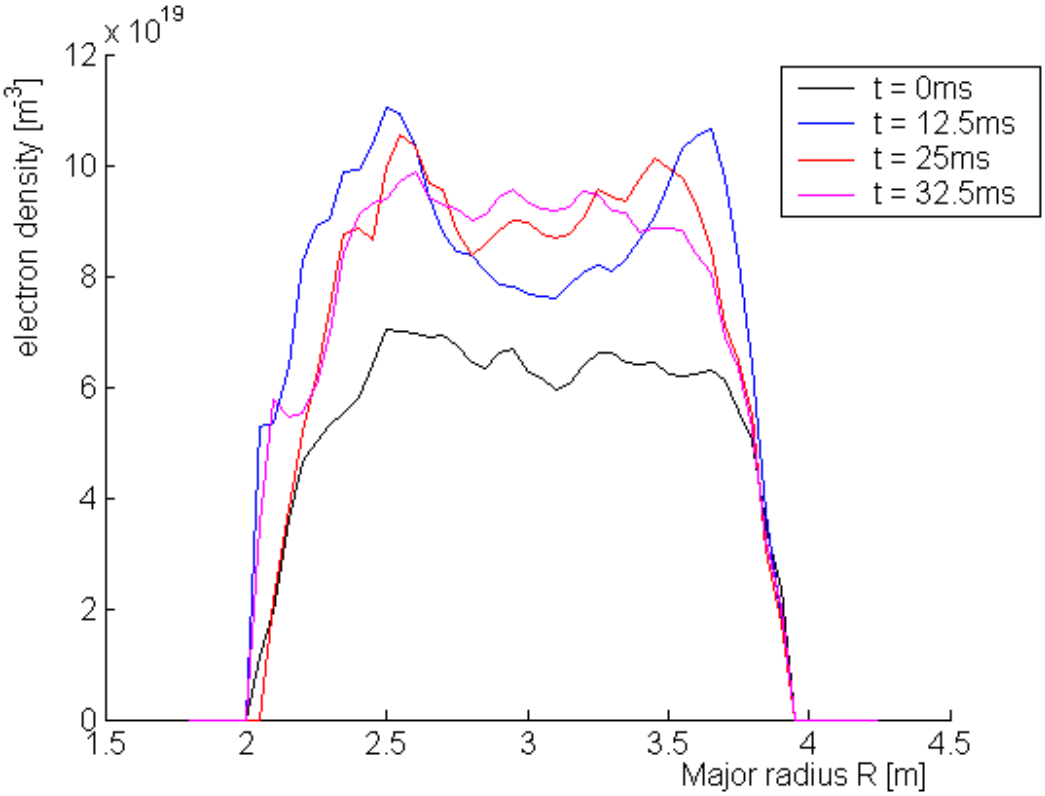

Figure3.1: Post pellet density profiles received from boxcar analysis in [2], which were used for the diffusion coefficient estimation. Relative time *0ms* marks the injection of the pellet (black).

Gaussian fit analysis

It is possible to estimate the diffusion coefficient D from the evolution of post pellet density perturbation $\delta n(R,t)$:

$$\delta n(R,t) = n(R,t) - n(R,0), \tag{3.7}$$

where R is the major radius and $n(R,0)$ is the density profile before the pellet injection. This method is based on the relationship between D and the width of the density perturbation. If we assume axial symmetry, the heat equation can be written in a following form:

$$\frac{\partial n}{\partial t} = D\left(\frac{\partial^2 n}{\partial r^2} + \frac{1}{r}\frac{\partial n}{\partial r}\right). \tag{3.8}$$

where $r=(x^2+y^2)^{1/2}$. One of the particular solutions of (3.8) has a gaussian shape [11]:

$$n(r,t) = A + \frac{B}{t}\exp\left(-\frac{r^2}{4Dt}\right), \tag{3.9}$$

where A,B are arbitrary constants. Therefore a fit of the post pellet density perturbation $\delta n(R,t)$ by a two-gaussian analytical expression (3.10) was done [10]:

$$\delta n(R,t) = A_i(t)\exp\left(\left(\frac{R-R_i(t)}{\Delta_i(t)}\right)^2\right) + A_o(t)\exp\left(\left(\frac{R-R_o(t)}{\Delta_o(t)}\right)^2\right), \tag{3.10}$$

where R is a major radius,

$$\Delta_{i,o} = \sqrt{4D_{i,o}t}\,, \tag{3.11}$$

indices i and o denote the fit of the inward and outward profile, as the density is perturbed on both HFS and LFS, as can be seen on *Fig.3.1*. The fit (3.10) was done for each of the three profiles at relative times after the pellet and therefore $A_{i,o}(t)$, $R_{i,o}(t)$ and $\Delta_{i,o}(t)$ are constants for the time t and are determined by the least square two-gaussian fitting process. The $\Delta_{i,o}(t)$ then allows us to compute inner and outer diffusion coefficients for the time t and $R_{i,o}(t)$ inform us about the position of the two (inner and outer) peaks of the perturbation.

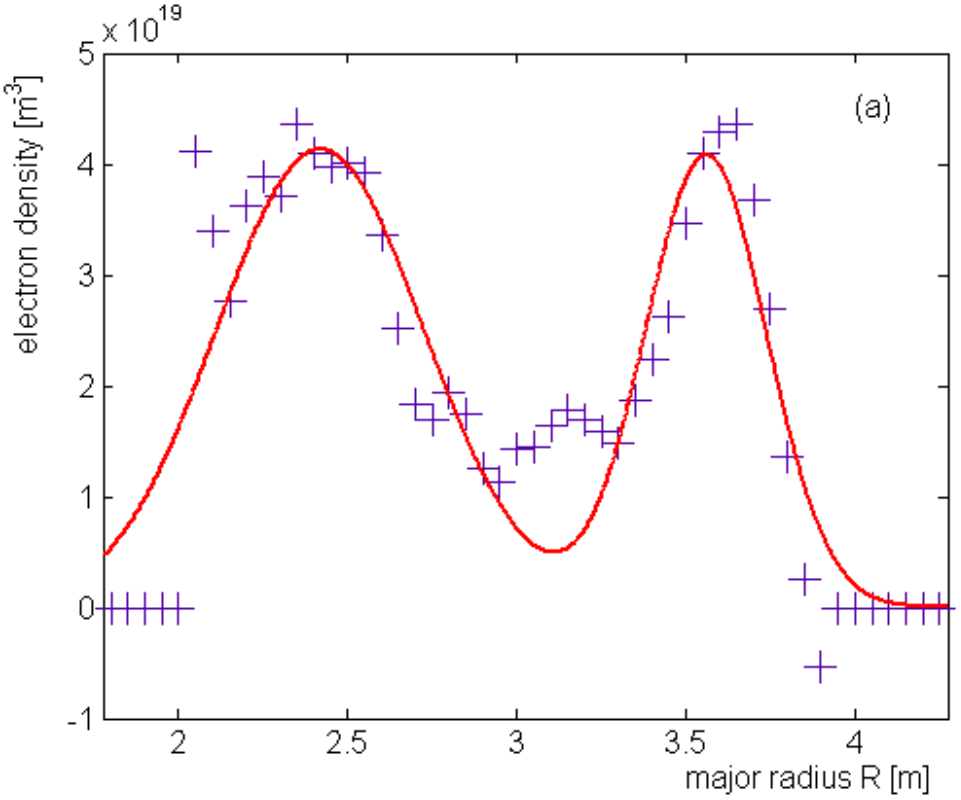
x 10^19
electron density [m^-3]
(a)
major radius R [m]

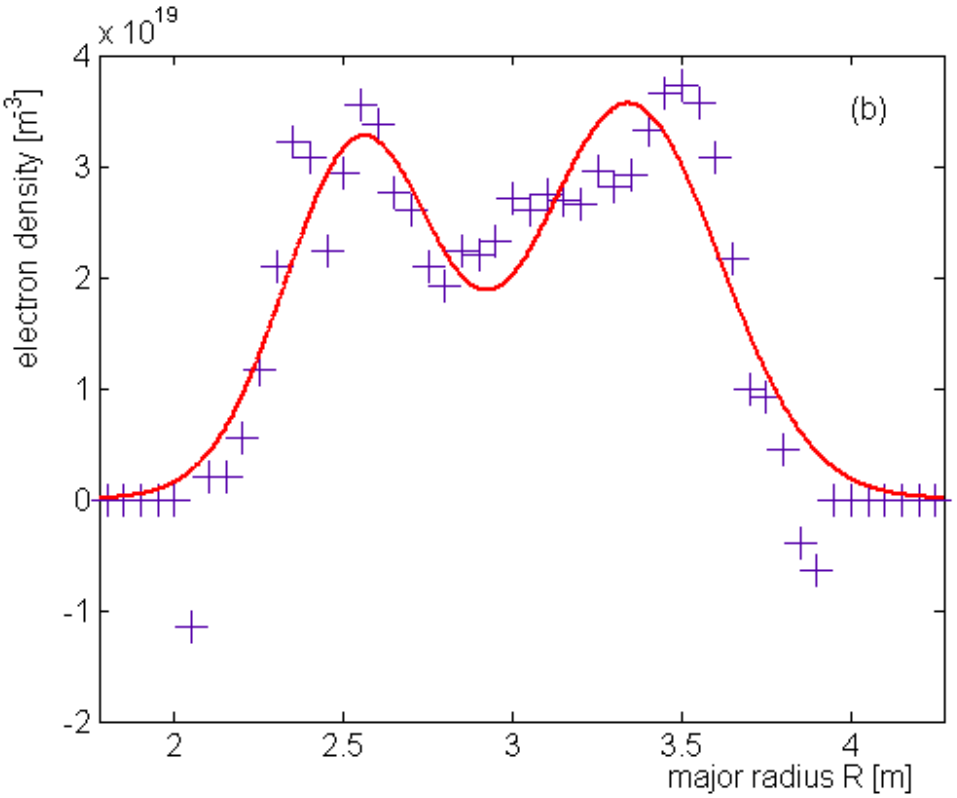
x 10^19
electron density [m^-3]
(b)
major radius R [m]

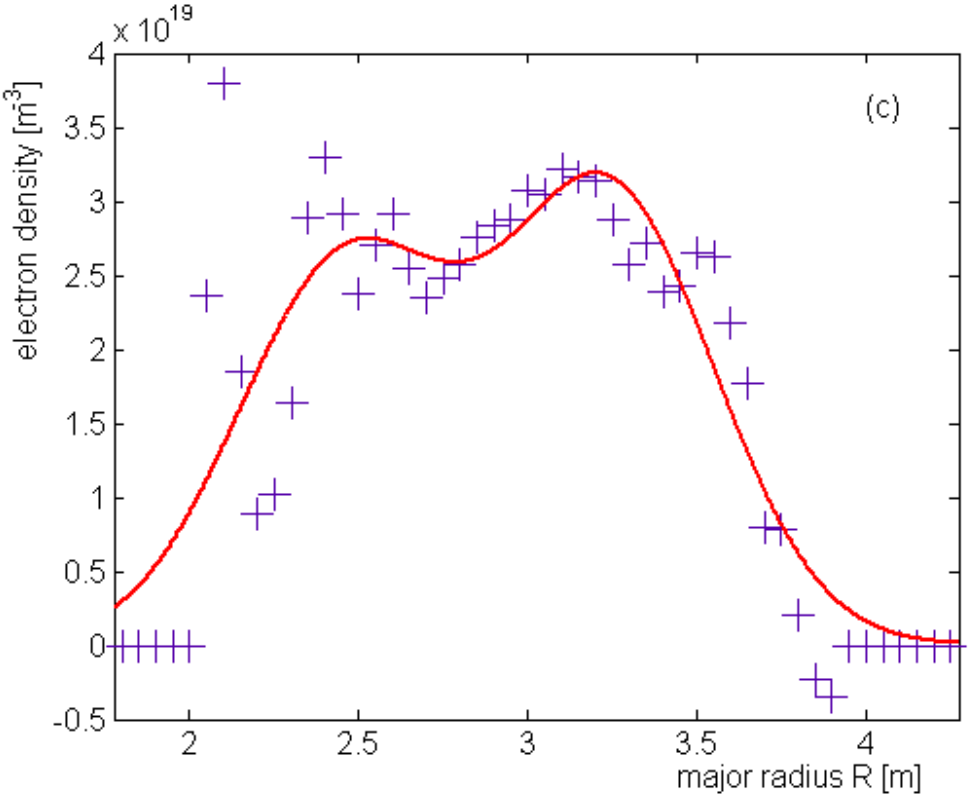

Figure3.2: The density perturbations δn after the pellet along with their two-gaussian fit for relative times *t=12.5ms* (a), *t=25ms* (b) and *t=32.5ms* (c).

The fitting was made with use of MATLAB 6.5 curve fittiing tool. The results are shown in *Tab.3.1* below. The coefficients of the fit are given with 95% confidence bounds.

Time [ms]	A_i [10^{19} m^{-3}]	A_o [10^{19} m^3]	R_i [m]	R_o [m]	Δ_i [m]	Δ_o [m]
12.5	4.13 ± 0.56	4.08 ± 0.72	2.42 ± 0.05	3.56 ± 0.04	0.43 ± 0.07	0.25 ± 0.05
25	3.22 ± 0.47	3.56 ± 0.43	2.56 ± 0.05	3.34 ± 0.05	0.32 ± 0.07	0.38 ± 0.08
32.5	2.57 ± 0.68	3.04 ± 0.73	2.46 ± 0.21	3.24 ± 0.18	0.45 ± 0.22	0.44 ± 0.17

Table3.1: Results of the two-gaussian fit of the density perturbation in times *t=12.5ms*, *t=25ms* and *t=32.5ms*.

From these data (*Tab.3.1*) it is possible to calculate the inner and outer diffusion coefficients $D_{i,o}$ (with use of (3.11)), and their average D_a. It is also possible to linearly fit $R_{i,o}$ versus time and by a time derivation of this fit to determine approximately a convective inward pinch of the deposited pellet $v_{i,o}$ (outer and inner again). This was not done, however, as the linear fit proved to be too inaccurate.

The results are given in *Tab.3.2* below:

Time [ms]	D_i $[m^2s^{-1}]$	D_o $[m^2s^{-1}]$	D_a $[m^2s^{-1}]$
12.5	**3.70 ± 1.20**	**1.25 ± 0.50**	**2.47 ± 1.30**
25	1.02 ± 0.44	1.44 ± 0.88	1.23 ± 0.99
32.5	1.56 ± 1.52	1.49 ± 1.15	1.52 ± 1.91

Table3.2: Diffusion coefficients at inboard and outboard side and their average calculated from the gaussian fit analysis of the post pellet data

The most important results are those immediately after the pellet evaporation, as they describe the fast post pellet losses. They are therefore highlighted in the *Tab.3.2* by a bold font.

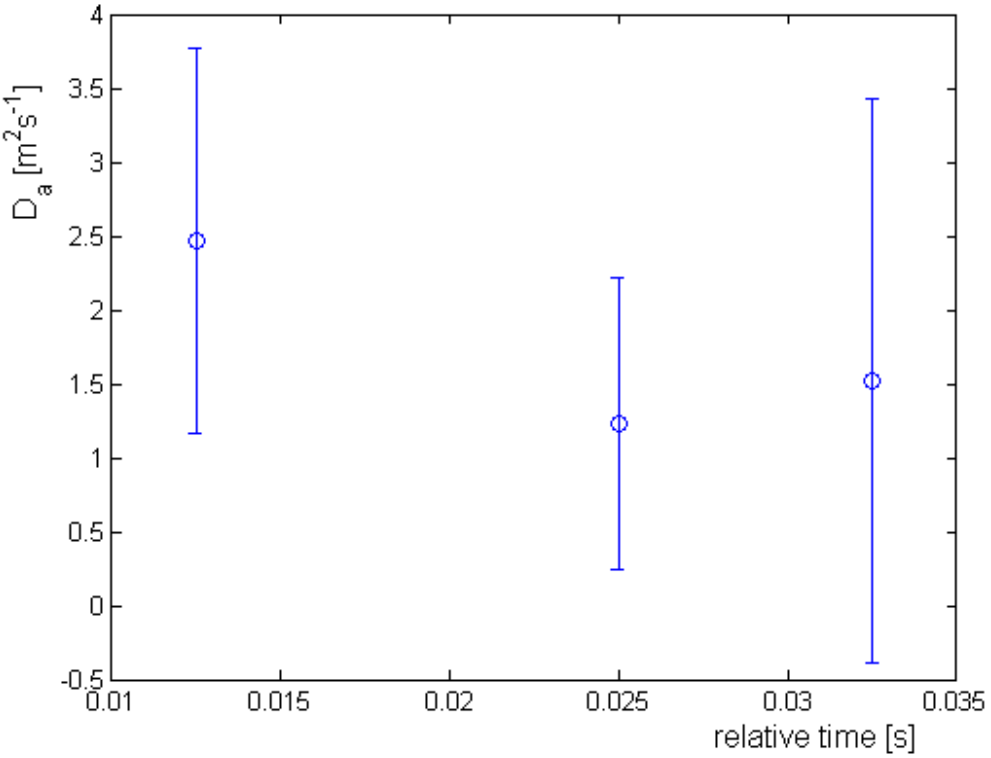

Figure3.3: The calculated average diffusion coefficient D_a after the pellet

Bessel functions analysis

The heat equation in axial symmetry (cyllindrical geometry) (7) with a general initial condition (2) and with boundaries $0 \le r \le L$ has a general solution of a form [11]:

$$n(r,t) = \int_0^R \alpha(\xi) G(r,\xi,t) d\xi \,, \tag{3.12}$$

where $G(r,\xi,t)$ is a Green's function. If a boundary condition $n=0$ for $r=L$ is prescribed, than the Green's function G can be written with use of Bessel functions as:

$$G(r,\xi,t)=\sum_{n=1}^{\infty}\frac{2\xi}{L^2 J_1^2(\mu_n)}J_0\left(\mu_n\frac{r}{L}\right)J_0\left(\mu_n\frac{\xi}{L}\right)\exp\left(-\frac{D\mu_n^2 t}{L^2}\right), \qquad (3.13)$$

where J_0 and J_1 are first order Bessel functions, defined as [6]:

$$J_m(x)=\sum_{k=0}^{\infty}\frac{(-1)^k}{k!(k+m)!}\left(\frac{x}{2}\right)^{2k+m}, \qquad (3.14)$$

and μ_n is the n-th positive zero of the Bessel function J_0 (which means $J_0(\mu_n)=0$).

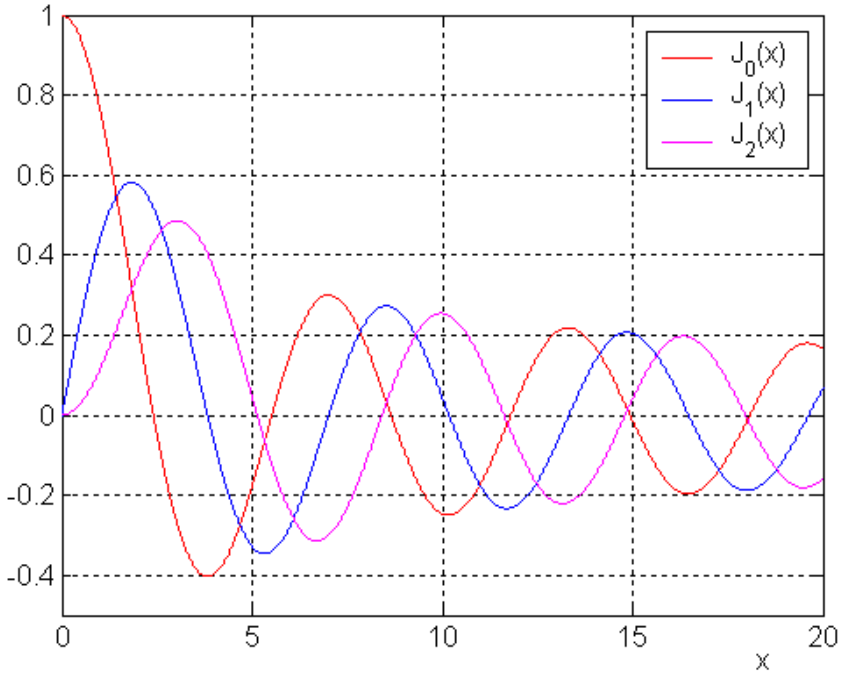

Figure3.4: The first three *first order Bessel functions* J_m.

To justify the use of axial symmetric heat equation the post pellet density perturbation profiles were averaged with respect to the tokamak minor (plasma) axis at $R \approx 3m$. Then these averaged profiles $\delta n(r,t)$ (for $0 \le r \le a$) were mapped on a 1-dimensional x grid varying between 0 and 1. $\delta n(x,t)$ in a new variable x were then fitted for each time t with a fourth degree polynomial $\delta\tilde{n}(x,t)$ to regularize the profile [10]. Then if $\delta\tilde{n}(x,t)$ is the initial condition at time t, with use of equations (3.12), (3.13) we may write for a solution at time $t+\delta t$:

$$\delta\tilde{n}(x,t+\delta t)=2\sum_{n=1}^{\infty}\frac{J_0(\mu_n x)}{J_1^2(\mu_n)}\exp\left(-D\mu_n^2\delta t\right)\int_0^1 J_0(\mu_n x)\delta\tilde{n}(x,t)x\,dx. \qquad (3.15)$$

The terms of the series on the right side of equation (3.15) fall down to smaller and smaller values with increasing *n*, therefore it is possible to cut off the series. A minimisation is then applied with respect to *D* of the term:

$$\sum_{i=1}^{N}\left(\delta\tilde{n}(x_i,t+\delta t)-\delta\hat{n}(x_i,t+\delta t)\right)^2=\left\|\delta\tilde{n}(x,t+\delta t)-\delta\hat{n}(x,t+\delta t)\right\|^2, \qquad (3.16)$$

where $\delta\tilde{n}(x,t+\delta t)$ is a function of *D* and is calculated from (3.15) and $\delta\hat{n}(x,t+\delta t)$ is the fourth degree polynomial fit of the density perturbation in time $t+\delta t$.

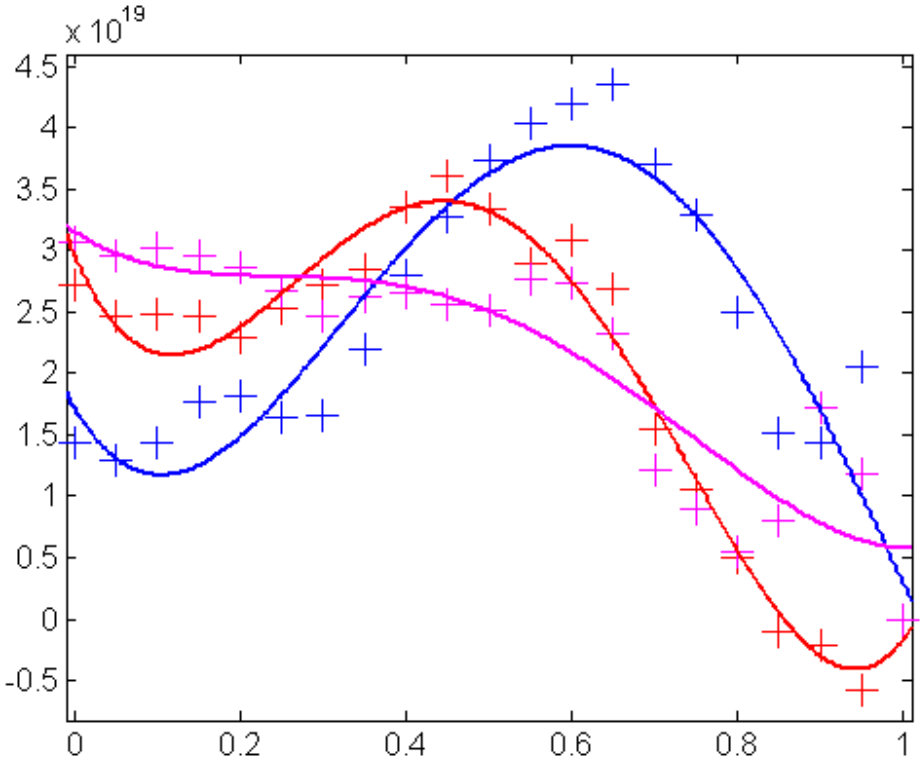

Figure3.5: The density perturbations *δn(x,t)* plotted in times *t=12.5ms* (blue), *t=25ms* (red) and *t=32.5ms* (magenta) in the new *x* coordinate (+ points) and their appropriate fourth degree polynomial fits in the same times (solid lines). The fitting was done by using MATLAB 6.5 curve fittng tool.

The fitted fourth degree polynomial $\delta\hat{n}(x,t)$ can be written in the following form:

$$\delta\hat{n}(x,t)=p_1x^4+p_2x^3+p_3x^2+p_4x+p_5, \qquad (3.17)$$

with constant coefficients $p_1 - p_5$. The results of the fitting are given in the *Tab.3.3* below (values are given with 95% confidence bounds):

Time [ms]	p_1 [10^{20}]	p_2 [10^{20}]	p_3 [10^{20}]	p_4 [10^{20}]	p_5 [10^{20}]
12.5	3.57 ± 3.96	-9.47 ± 7.99	6.90 ± 5.26	-1.15 ± 1.25	0.17 ± 0.09
25	8.07 ± 1.99	-16.19 ± 4.02	9.40 ± 2.64	-1.59 ± 0.63	0.30 ± 0.04
32.5	1.89 ± 3.80	-3.74 ± 7.66	2.05 ± 5.04	-0.46 ± 1.19	0.32 ± 0.08

Table3.3: Results of the fourth degree polynomial fit of the density perturbation $\delta n(x,t)$ in times *t=12.5ms*, *t=25ms* and *t=32.5ms*.

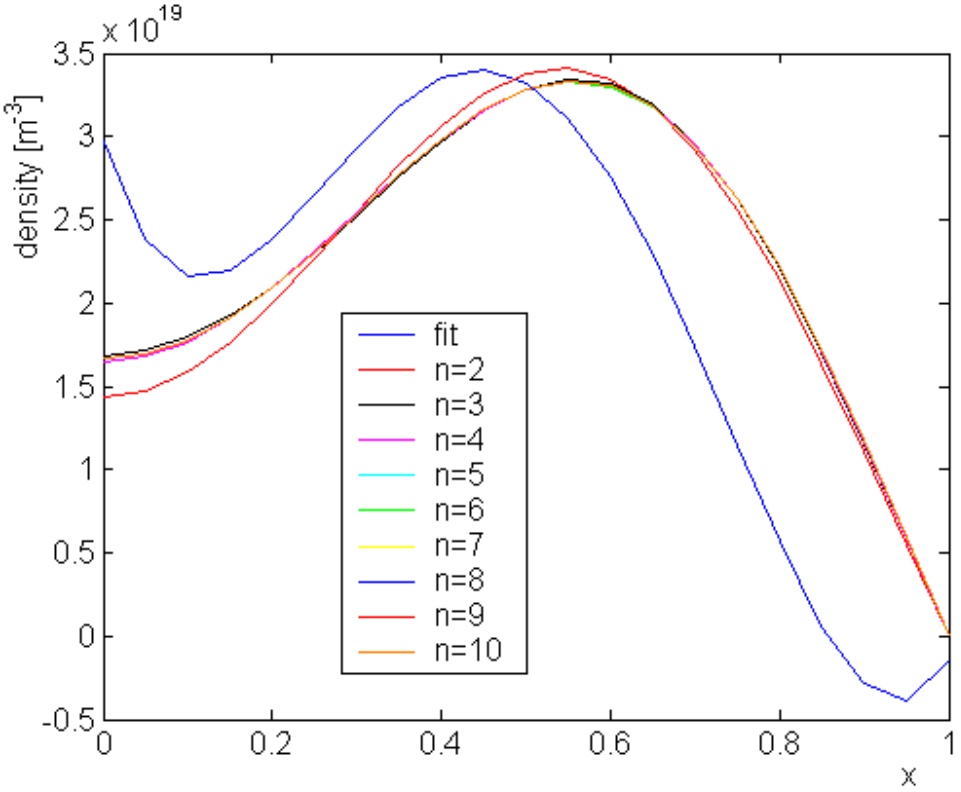

Figure3.6: The results $\delta\tilde{n}(x,t+\delta t)$ of summation (3.15) for different considered number *n* of the series for times *t=12.5ms* and $t+\delta t$*=25ms* and with use of an expected value of $D=1m^2s^{-1}$. The fourth degree fit of the density perturbation $\delta n(x,t+\delta t)$ in time $t+\delta t$*=25ms* is given to compare (blue).

On *Fig.3.6* are given the results $\delta\tilde{n}(x,t+\delta t)$ of summation (3.15) for different considered number *n* of the summed terms for times *t=12.5ms* and $t+\delta t$*=25ms* and with use of an expected value of $D=1m^2s^{-1}$. It can be seen, that there is not an observable difference between functions, which come up from the series in (3.15) cut off at $n \geq 3$. For this particular calculation, the series was cut off for n > *10*. This can be defended by the fact that for values of *D* not too near to zero

the contribution of the last term in the sum was reduced to less than 1% (more precisely the value of maximum difference between the functions, which come up from the series cut off at n=11 and n=10, was reduced to less than 1% of the average value of the function for n=10). The minimisation process was then performed, for $0 < D \leq 10\ m^2s^{-1}$. The results of the Bessel functions analysis are given in *Tab.3.4* below:

Time window	***D [m^2s^{-1}]***
12.5 ms - 25 ms	3.295
25 ms – 32.5 ms	2.872

Table3.4: Diffusion coefficients calculated by the Bessel functions analysis

3.3 Pellet particle confinement

As the pellets are injected into the plasma and reach deeper regions of the plasma column before total evaporation, they greatly affect the plasma confinement and transport, especially at the edge. The local density increase can be in order of tens of percent (for ITER could be up to 50%, depending on the penetration) and the plasma is non-stationary, responding to these perturbations. The main parameters of the pellet, which affect the post pellet transport, are the *pellet deposition radius* r_{pel} and *post pellet particle confinement time* (pellet retention time) τ_{pel}. These two parameters are very important, because they determine the particle throughput provided by the pellet injection system, which is necessary to maintain the plasma density:

$$\Phi_{pel} \approx n_e S\,(a-r_{pel})/\tau_{pel}, \qquad (3.18)$$

where n_e is the electron density averaged in time (over pellets) and radius $r_{pel} \leq r \leq a$, S is the plasma surface.

The *pellet deposition radius* is a radius, where the major part of the pellet evaporates and is deposited. It depends on the injection speed, pellet size, pellet injection path and additional effects like pellet grad$B$ drifting and plasma turbulence. The pellet evaporation for JET shot 53212 lasts usually about 10ms. For our case, the pellet deposition radius can be determined from the post pellet electron density profile.

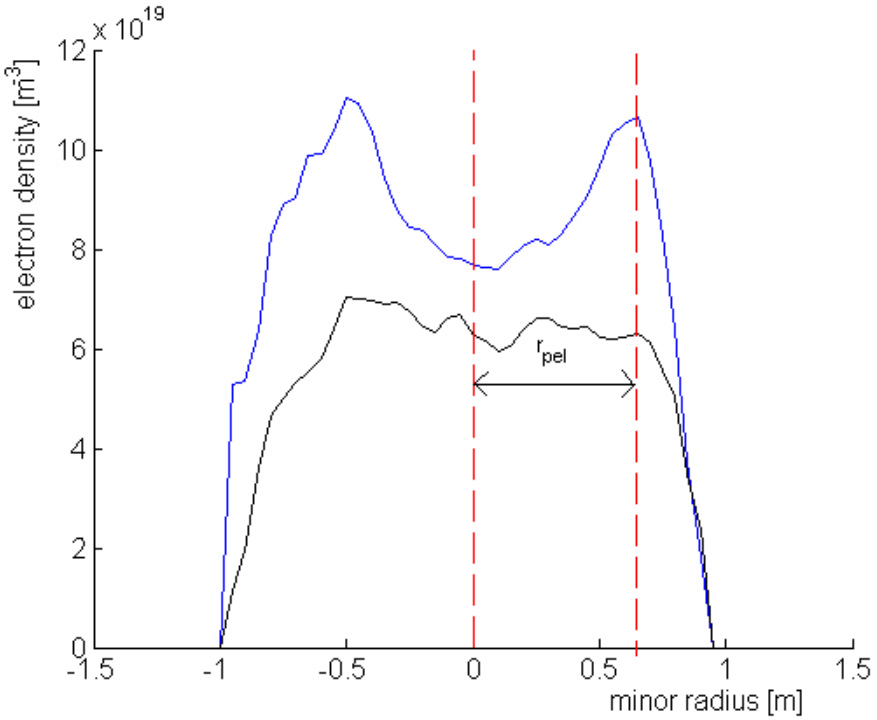

Figure3.7: Electron density profile 5ms after the pellet evaporation (blue), electron density profile before injection is given for comparation (black)

From *Fig.3.7* it is possible to approximately determine the pellet deposition radius r_{pel}. The interval of radii, where the most particles are deposited is about $r \in (0.45m, 0.75m)$ (on the outer edge of plasma), therefore $\boldsymbol{r_{pel} \approx 0.6m}$.

The pellet injection induces a strong perturbation of the plasma and affects the confinement significantly. The development of the edge plasma transport after the pellet is described by the *post pellet particle confinement time* τ_{pel}. It can be determined from the post pellet evolution of plasma density at a fixed radius:

$$n_e(t,r_{pel}) \propto exp[-(t-t_{pel})/\tau_{pel}] \qquad (3.19)$$

where t_{pel} is a time of the total pellet evaporation (deposition). From the equation (3.19) it can be seen, that τ_{pel} represents a characteristic time of the perturbed density evolution. The calculation can be made by taking a logarithm of the equation (3.19) and doing a linear least sqare fit of the data.

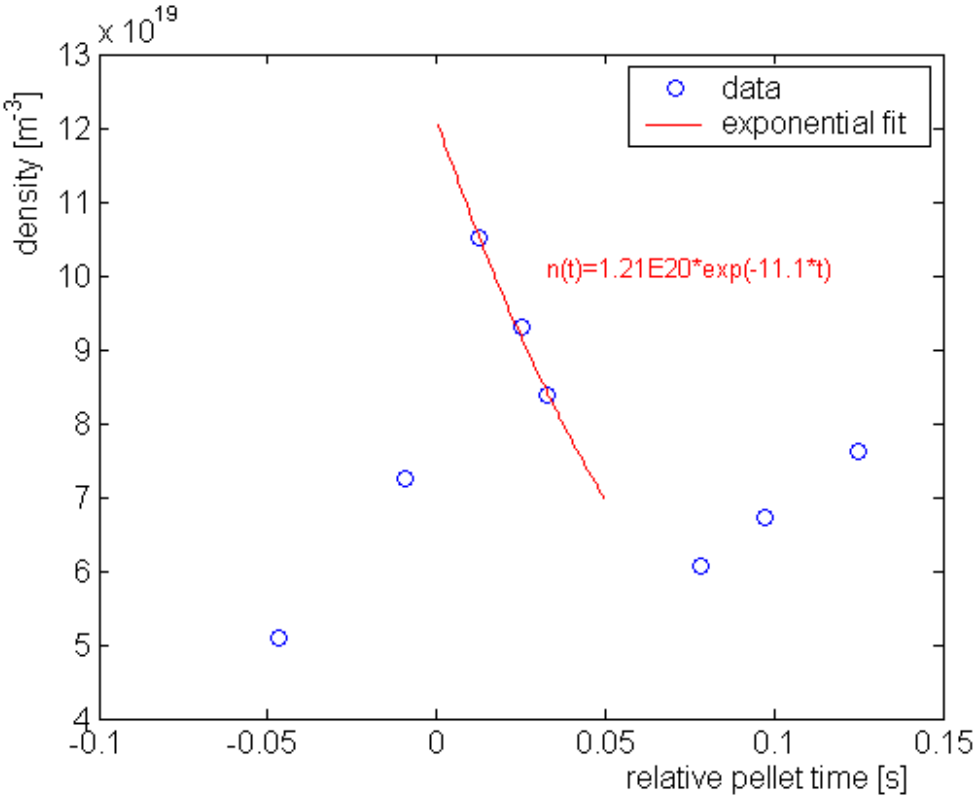

Figure3.8: Exponential fit of the post pellet density evolution at pellet deposition radius r_{pel}=*0.6m*
The data used are from [2] (see *Fig.3.14*)

With use of the pre-processed data from [2] (see *Fig.3.14*) the exponential fit was done for the relative time interval *(0s,0.05s)*, where *t=0s* means the moment of pellet injection. The time interval was chosen only for the short post-pellet interval in order to compute the immediate quick losses of the plasma particles. The fitted density-time dependance is:

$$n_e\left(t, r_{pel}\right) = 1.21 \cdot 10^{21} \exp\left[-11.1 \cdot \left(t - t_{pel}\right)\right] \qquad (3.20)$$

Therefore the value of τ_{pel}, along with its standard error from the log-linear fit is:

- $\boldsymbol{\tau_{pel} = 90.3 \pm 7.7 ms}$

This value corresponds with the typical values of pellet retention time during the JET discharges, which is about 50 – 100ms.

For a more precise calculation in order to exclude density changes due to gas puffing and NBI it would be desirable to modify the left side of equation (3.19) by substracting the density, which would have occured without the pellet (determined by a linear extrapolation of pre-pellet data). This was not done in this case due to insufficiency of relevant pre-pellet data, however, from the pre-pellet density evolution measured by interferometer (see [2] *Fig.3.2, Fig.3.12*) it is possible

to assume the resulting error as negligible. Another possible error of this calculation arises from the fact, that the density evolution need not have an exponential shape and that the τ_{pel} is not a constant, but changes in time and is usually shorter immediately after the pellet than later on. To minimize this, only a short time interval of fast particle losses was chosen for the calculation. The error may be also enhanced by the insufficient data for this particular analysis and by the error of the boxcar method itself [2].

If we carry out a dimensional analysis of the simplified diffusion equation (3.1), where D is the particle diffusion coefficient, and we assume a characteristic time of the density evolution to be τ_{pel} and a characteristic length to be pellet penetration depth, which is $\Delta_r = a - r_{pel}$, we get:

$$\frac{n}{\tau_{pel}} \propto \frac{n}{\Delta_r^2} \tag{3.21}$$

and we can express τ_{pel} in the following form:

$$\tau_{pel} = \text{const.} \cdot (\Delta_r^2 / D), \tag{3.22}$$

or in a form more suitable for scaling purposes:

$$\tau_{pel} = \text{const.} \cdot a^2 \cdot ((1-\rho_{pel})^2 / D), \tag{3.23}$$

where $\rho_{pel} = r_{pel}/a$ is the pellet deposition radius normalized to the minor radius. The constant in (3.22), (3.23) depends on the exact shape of the density profile. From the knowledge of D and τ_{pel} it is possible to approximately determine the constant for our experiment and gain a useful and simple formula $\boldsymbol{\tau_{pel} \approx (0.6\text{-}0.9) \cdot (\Delta_r^2 / D)}$ (For diffusivity D we used the computed values $D = 0.8 \pm 0.4\ m^2 s^{-1}$ found in [2] and $D = 1.25 \pm 0.5\ m^2 s^{-1}$ found in the gaussian fit analysis in chapter 3.2 for the outer edge of plasma – see *Tab.3.2*).

To be able to predict the pellet retention time τ_{pel} to next step devices such as ITER, the experimental values are usually normalized to the total energy confinement time τ_E, for which there exist an energy confinement scaling. The energy confinement time is defined as the total energy content of the plasma divided by the total power input. For JET shot 53212 during the pellet operation $E \approx 5\text{-}6MJ$, $P \approx 18MW$ and so $\tau_E \approx 0.28\text{-}0.33s$.Therefore $\boldsymbol{\tau_{pel} / \tau_E \approx 0.27\text{ -}0.33}$. The pellet retention time is normalized to the energy confinement time because of an assumption, that the two processes of particle and energy transport are bounded and both heat and particle transport after the pellet is driven by the same turbulence. Usually, the diffusion coeficient D and heat transport coefficient χ follow a relation $D \approx (0.2\text{-}0.6)\,\chi$.

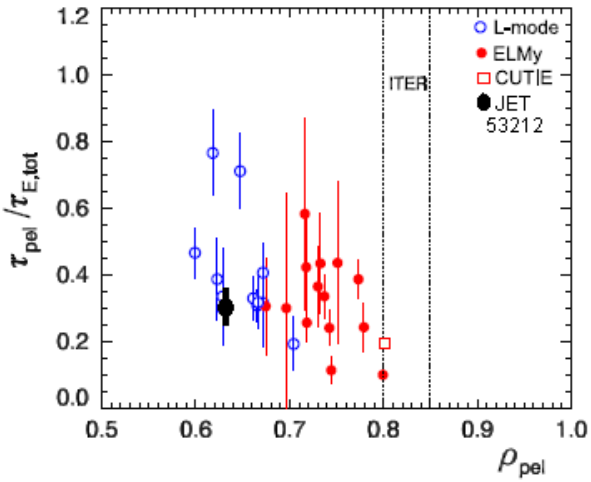

Figure3.9: Comparison of the ratio τ_{pel}/τ_E for JET shot 53212 (black) and for experiments on MAST tokamak [4]

On *Fig.3.9* can be observed, that the ratio τ_{pel}/τ_E for JET corresponds well with similar measurement made for the MAST tokamak.

In this chapter I used information from [4].

3.4 Post pellet plasma fluctuations

As can be seen from *Tab.3.2, Tab.3.4* the post pellet diffusion coefficient is anomalous, as it reaches values ~1m^2s^{-1}. A simple estimate was therefore made to roughly determine the size of the plasma turbulent fluctuations, which would cause this enhanced anomalous transport after the pellet injection.

The post pellet particle flux can be estimated with knowledge of the effective diffusion coefficient D_{eff} from the equation (2.5). D_{eff} was determined in [2] as ~ 0.8m^2s^{-1} and in the gaussian fit analysis in chapter 3.2 as ~ 1.25 m^2s^{-1} (see *Tab.2*), both these values being for the outer edge of plasma (LFS) and describing the fast post pellet losses (12.5ms after the pellet injection and 5ms after the pellet total evaporation). The gradient in (2.5) can be approximated for the edge plasma by:

$$grad \sim 1/(r_{pel} - a), \tag{3.24}$$

where r_{pel} is the pellet deposition radius and a is the plasma minor radius (see *Fig.3.4*). Therefore the simplified equation suitable for numerical evaluation of the edge plasma particle flux after the pellet injection takes following form:

$$\Gamma = D_{eff}\, n/(a - r_{pel}), \tag{3.25}$$

where n is the plasma density, which is taken for radius r_{pel} and time $t=12.5ms$ after the pellet (the right peak of the density profile on *Fig.3.7*). With the knowledge of r_{pel} ~ 0.6m and a ~ 0.95m, the post pellet particle flux Γ is evaluated for the outer edge plasma*:*

- $\Gamma \approx 3 \cdot 10^{20}\ m^{-2}s^{-1}$

electrostatic fluctuations

At first we assume this flux to be caused by electric field fluctuation (perpendicular to the magnetic field) (2.8),(2.9). The typical density fluctuations at the edge plasma are $\delta n/n \sim 0.1$. For a fluctuation of the electric field we may write:

$$\delta E = grad\ \delta\phi\,, \tag{3.26}$$

where $\delta\phi$ is a fluctuation of the plasma electric potential. In the equation (3.26) the gradient operation can be approximated by multiplying by the typical wavenumber of the fluctuations, perpendicular to the magnetic field k_{perp}. This wavenumber is related to the ion Larmor radius $r_{L,i}$, as it is usually $k_{perp} \cdot r_{L,i}$ ~ 0.4. The equation (2.9) may be rewritten in the following form:

$$\Gamma = <\delta v_{perp} \cdot \delta n> = \delta v_{perp} \cdot \delta n \cdot cos\,\theta, \tag{3.27}$$

where on the right side there are the sizes of the fluctuations and θ is the angle between those two fluctuations. Therefore we may write with use of (3.26), (3.27), (2.8)

$$\delta\phi = \frac{2.5 \cdot r_{L,i} B_T}{n\left(\frac{\delta n}{n}\right)\cos\theta}\Gamma\,, \tag{3.28}$$

where the constant *2.5* comes up from the relation between k_{perp} and $r_{L,i}$. The ion Larmor radius $r_{L,i}$ is determined by a formula:

$$r_{L,i} = \frac{m_i v_{perp,i}}{eB_T}\,, \tag{3.29}$$

where $v_{perp,i}$ is the ion velocity perpendicular to the magnetic field, e is the ion electric charge and m_i is the ion mass. By assuming the velocity to be thermal and the ion temperature to be approximately equal to the electron one $T_i \approx T_e$ we may write:

$$v_i \approx \sqrt{\frac{kT_e}{m_i}} \text{ and } \delta\phi = \frac{2.5 \cdot \sqrt{m_i kT_e}}{en\left(\frac{\delta n}{n}\right)\cos\theta}\Gamma \tag{3.30), (3.31}$$

where T_e is the electron temperature and k the Boltzmann constant. For a numerical calculation, folowing values were used: $m_i = 3.33 \cdot 10^{-27} kg$ is the mass of deuteron (assuming deuterium

plasma), $kT_e \approx 1.3keV$ is the plasma electron temperature for given time after the pellet and for radius r_{pel}, $e=1.6\cdot10^{-19}C$ is the elementary charge, $n \approx 10^{20}m^{-3}$ is the plasma electron density for the same time and radius as the temperature, $\delta n/n \sim 0.1$ and $\cos\theta \sim 1/3$. The resultant potential fluctuation $\delta\phi$ therefore is:

- $\boldsymbol{\delta\phi \approx 1.2\ V}$

It is usual to relate $e\delta\phi$ to kT_e, as $e\delta\phi$ is usually a small part of the electron temperature kT_e,. For our case:

- $\boldsymbol{e\delta\phi \approx 0.001\ kT_e}$

magnetic fluctuations

From *Fig.3.10, Fig.3.11* below, which show the interferometer line averaged plasma density and the D_α emission during the pellet operation [2] it is obvious, that ELM's play crucial role and are the major reason for post pellet fast particle losses.

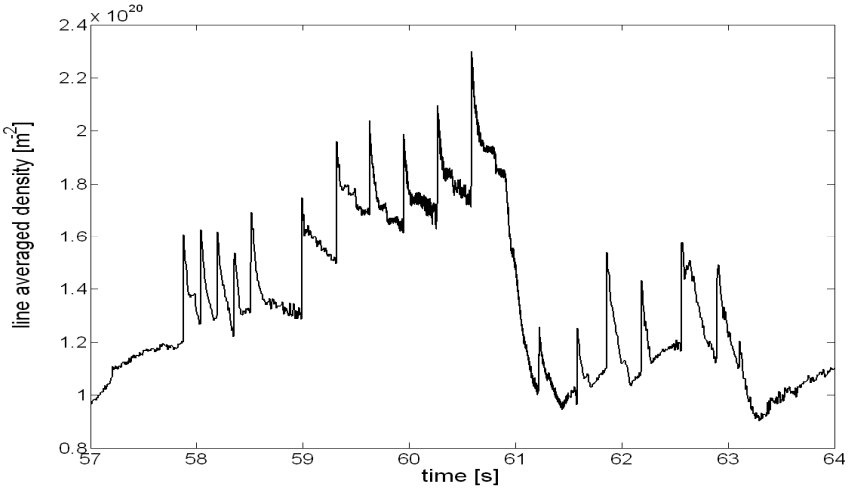

Figure3.7: Line averaged plasma density measured by chord 8 during the pellet operation (taken from [2] – *Fig.3.2*)

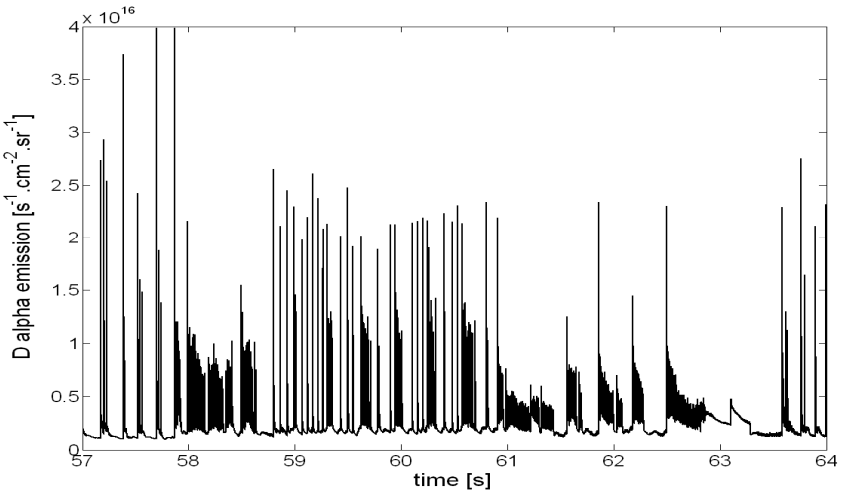

Figure3.8: D_α emission during the pellet operation (taken from [2] – *Fig.3.4*)

ELM's are magnetohydrodynamic (MHD) instabilities, which affect the magnetic field. From this it is possible to deduce that the anomalous transport due to magnetic fluctuations and disturbance of the magnetic field may be more relevant than the anomalous transport driven by electrostatic fluctuations.

The value of radial magnetic field fluctuation δB_r, which would cause the post pellet transport of particles may be roughly estimated using equations (2.21), (2.22) (note that it can be used only when assuming collisionless plasma, where $\lambda > L_c$). We assume $v_{par} \approx c_s$, where c_s is the speed of sound for ions in plasma [6]:

$$c_i = \sqrt{\frac{\gamma_i k T_i}{m_i}}, \tag{3.32}$$

where γ_i is the polytropic index for ions, k is the Boltzmann constant, T_i the ion temperature and m_i the ion mass. Equation (2.22) can be then written in the following form:

$$D = c_s \left(\frac{\delta B_r}{B} \right)^2 L_c \Rightarrow \delta B_r = B \sqrt{\frac{D}{L_c c_s}}. \tag{3.33}$$

With use of estimates $L_c \sim qR \sim 10m$, $T_i \approx T_e$ and using following values: $m_i = 3.33 \cdot 10^{-27} kg$, $B = 2.4T$, $\gamma_i \approx 5/3$, $kT_e \approx 1.3keV$, $D \approx 1 m^2 s^{-1}$ the radial magnetic field fluctuation δB_r, which would cause the post pellet particle transport, was roughly determined as:

- $\boldsymbol{\delta B_r \approx 1.3mT}$

4 Summary

In this work, the particle confinement of pellet fuelled plasmas in tokamaks was investigated. Plasma refuelling is one of the most important parts of the tokamak research. The most important technology of tokamak plasma fuelling for future devices like ITER would be pellet injection. The question of refuelling is also closely connected with the energy and particle confinement and transport in plasma. The confinement of the toroidally symmetric tokamak plasma has been calculated for particle Coulomb collisions. This so called neoclassical transport does not, however, agree with the experiments. The real transport in tokamaks, which is higher than the neoclassical predictions, is called anomalous. To explain and understand the theory of anomalous transport is one of the major challenges for present tokamak physics.

In the teoretical part of this work the basics of transport in tokamaks, mainly the anomalous one are given. The turbulence-driven anomalous transport is caused by fluctuations of the plasma. These fluctuations may be electrostatic or electromagnetic and are supposed to be an effect of one or more microinstabilities of the tokamak plasma. Macroscopic MHD instabilities like sawteeth, magnetic islands or ELMs are also an important source of the anomalous transport.

The experimental part of this work is based upon previous bachelor thesis [2], where a post pellet particle diffusion coefficient was calculated. The data used in this work are from the JET shot 53212, which was a part of experiments undertaken at JET aimed to develop optimized pellet refuelling scenarios. The first step was to perform a more profound analysis of the post pellet transport than in [2]. Two ways of analysing the post pellet data were used to compute the edge plasma effective diffusion coefficient: gaussian fit analysis and Bessel functions analysis. The gaussian fit method was based on the relationship between *D* and the width of the density perturbation after the pellet. The density perturbation was fitted by a two-gaussian analytical expression and the resulting inner and outer diffusion coefficients were in good agreement with the expected values. In the Bessel functions analysis, the general solution of the diffusion equation in axial symmetry was used. The resultant post pellet diffusion coefficients are also reasonable and confirm the previous results. Generally the diffusion coefficients for the edge plasma after the pellet are of the order of $\sim 1 m^2 s^{-1}$.

In the next chapter the pellet retention time and the pellet deposition radius were estimated. The pellet retention time is a characteristic time of the post pellet density evolution, the pellet deposition radius is a radius, where the major part of the pellet evaporates and is deposited. These two parameters are very important, as they determine the particle throughput provided by the pellet injection system, which is necessary to maintain the plasma density. They were determined as $\tau_{pel} = 90.3 \pm 7.7 ms$ and $r_{pel}=0.6m$. The pellet retention time was then normalized by the energy confinement time and compared with similar results from the MAST tokamak.

The last task was to estimate the post pellet plasma fluctuations which drive the anomalous transport. Assuming the post pellet transport to be caused by electrostatic fluctuation it was possible to roughly determine the plasma potential fluctuations: $e\delta\phi \approx 10^{-3} kT_e$. From the enhanced D_α emission during the pellet operation and its correlation with the quick transport phases it can be deduced, however, that the anomalous transport driven by the perturbation of the magnetic field structure by ELM's may be more relevant. Radial magnetic field fluctuation δB_r, which would cause the post pellet particle transport, was roughly determined as $\delta B_r \approx 1.3 mT$.

5 References

[1] *ITER* [online]. [cit. 2008-09-13] <http://www.iter.org>

[2] P.Háček. *Fuelling efficiency and its impact on plasma parameters in tokamaks*, Bachelor thesis. FJFI ČVUT v Praze, 2007

[3] J.Wesson. *Tokamaks, third edition*. Oxford University Press, Clarendon Press, Oxford, 2004

[4] M. Valovič et al. *Particle confinement of pellet-fuelled tokamak plasma*. Nucl. Fusion 48 (2008) 075006 (8pp)

[5] E.J.Doyle et al. *Chapter 2: Plasma confinement and transport.* Nucl. Fusion 47 (2007) S18 – S127

[6] P. Kulhánek. *Teorie plazmatu*, studijní text pro FJFI ČVUT, [online]. [cit. 2008-09-14] <http://www.aldebaran.cz/studium/fpla.pdf>

[7] H. W. Barthels, H.S. Bosch, R. Brakel, H.J. Hartfuss, D. Hartmann, R.Hippler, D.H.H. Hoffmann, R. Kleiber, A. Könies, K. Krieger, A. Melzer,A.G.Peeters, R. Schneider, B.D. Scott, W. Suttrop, H. Zohm. *IPP Summer University for Plasma Physics*, Greifswald, 2005

[8] Milan Krbálek. *Úlohy matematické fyziky, cvičení.* FJFI ČVUT v Praze, 2008

[9] *Heat equation – Wikipedia, the free encyclopedia* [online]. [cit. 2008-09-17] <http://en.wikipedia.org/wiki/Heat_equation>

[10 Luca Garzotti. *Post pellet injection transport analysis on MAST.* April 25, 2007

[11] Andrei D. Polyanin, Alexander V. Manzhirov. *Handbook of mathematics for engineers and scientists.* CRC Press, 2007

6 Acknowledgements

I would like to thank to my supervisor Ing. Martin Valovič, Ph.D, who helped me greatly with this work and did not lose temper, as the main part of the work was done at the eleventh hour. I would also like to thank to my consultant Ing. Ivan Ďuran, Ph.D, who willingly aided me always when I was in problems.